Eur. Phys. J. A **6**, 377–380 (1999)

THE EUROPEAN PHYSICAL JOURNAL A
© Springer-Verlag 1999

Short note

The 3701 keV neutron $g_{9/2}$ single-particle state in ^{57}Ni

D. Rudolph[1], D. Weisshaar[2], F. Cristancho[3,4], J. Eberth[2], C. Fahlander[1], O. Iordanov[3], S. Skoda[2], Ch. Teich[3,a], O. Thelen[2], H.G. Thomas[2]

[1] Department of Physics, Lund University, 22100 Lund, Sweden
[2] Institut für Kernphysik, Universität zu Köln, 50937 Köln, Germany
[3] II. Physikalisches Institut, Universität Göttingen, 37073 Göttingen, Germany
[4] Departamento de Física , Universidad Nacional de Colombia, Bogotá, Colombia

Received: 24 September 1999 / Revised version: 22 October 1999
Communicated by D. Schwalm

Abstract. The neutron $g_{9/2}$ single-particle state in ^{57}Ni has been unambiguously identified in a combined measurement of the linear polarization, angular distribution, and angular correlation of γ rays following the fusion-evaporation reaction ^{28}Si(^{32}S,2pn)^{57}Ni at a beam energy of 90 MeV. The linear polarization was measured with a EUROBALL cluster detector and a prototype of an encapsulated six-fold segmented hexaconical Ge-detector. The spin of the 3701 keV level in ^{57}Ni was confirmed to be $I = 9/2$ and its parity determined to be positive.

PACS. 21.10.Hw Spin, parity, and isobaric spin – 21.60.Cs Shell model – 23.20.En Angular distributions and correlation measurement – 27.40.+z $39 \leq A \leq 58$

The knowledge of the single-particle energies in the vicinity of doubly-magic nuclei is of great importance in low-energy nuclear structure studies. For any nuclear many-body model single-particle energies are either vital parameters (e.g., in the shell-model) or reflect basic bench-marks (e.g., for mean-field calculations). Around ^{56}Ni, the positions of the negative-parity orbits $1f_{7/2}$, $2p_{3/2}$, $1f_{5/2}$, and $2p_{1/2}$ are well established from either particle- or γ-spectroscopic investigations of the odd-A one-hole and one-particle neighbours ^{55}Co and ^{55}Ni [1], and ^{57}Ni and ^{57}Cu [2], respectively. The positive-parity orbits from the *sd*-shell, located below ^{40}Ca, are known or suggested in the $A = 55$ mirror system [1], but they do not play a significant role for the high-spin states in or above ^{56}Ni. Instead, the description of, e.g., the recently observed rotational bands just above ^{56}Ni [3,4] calls for the occupation of the positive-parity $1g_{9/2}$ high-j intruder orbit. The single-particle energy of the $1g_{9/2}$ shell around ^{56}Ni remains to be determined, though a promising candidate, namely the 3701 keV $I = 9/2$ state in ^{57}Ni, has been put forward recently [5].

Figure 1 provides the important part of the proposed high-spin excitation scheme of ^{57}Ni: The 3701 keV level was found to decay via the 1124 keV stretched $\Delta I = 1$ transition into the $7/2^-$ yrast state, and through the 2933 keV transition into the $1f_{5/2}$ single-particle state at 768 keV. Mainly two arguments were put forward to sug-

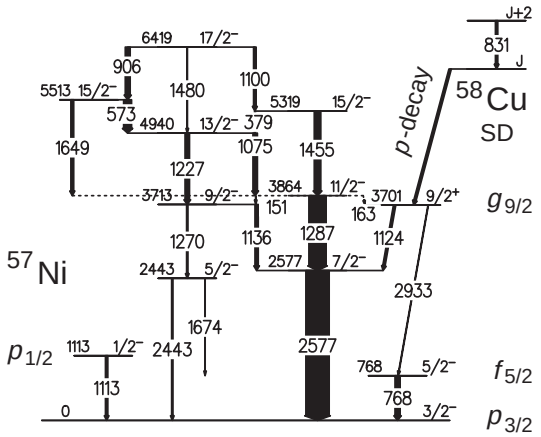

Fig. 1. Partial experimental level scheme of ^{57}Ni [2,5]. The energy labels are given in keV. The widths of the arrows indicate the relative intensities of the γ rays. On the right hand side, the beginning of the proton-emitting, strongly deformed band in ^{58}Cu [4] is sketched. The ground-state and the levels at 768 and 1113 keV have previously been interpreted as $p_{3/2}$, $f_{5/2}$, and $p_{1/2}$ single-particle states with respect to the ^{56}Ni core (e.g., [6,7]). The level at 3701 keV excitation energy is the one of interest

[a] *Present address:* Robert Bosch GmbH, Stuttgart, Germany

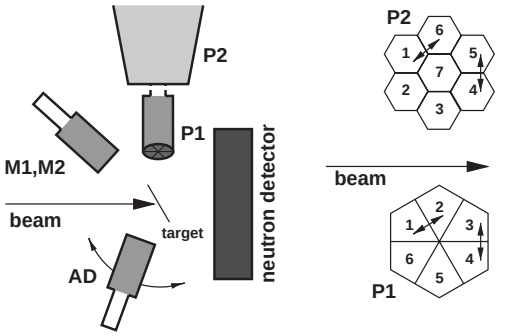

Fig. 2. Sketch of the experimental set-up. For details see text

gest a positive parity for the 3701 keV level. Firstly, the bare existence of the nearby $I^\pi = 9/2^-$ level at 3713 keV — another $I^\pi = 9/2^-$ state only 12 keV apart implies a nearly orthogonal wave function which is difficult to accomodate theoretically [5]. Secondly, it represents the daughter state of the exotic prompt proton decay of the deformed band in ^{58}Cu [4]. The band is considered to be built on a deformed $[\pi\, 1g_{9/2} \otimes \nu\, 1g_{9/2}]$ configuration with the $1g_{9/2}$ proton being emitted. Nevertheless, the spin and parity of the band head in ^{58}Cu is yet to be determined, which, in turn, adds one more argument why it is important to fix the parity of the daughter state in ^{57}Ni.

The experiment was performed at the Tandem accelerator of the University of Cologne in Germany. The set-up is sketched in Fig. 2. The 90 MeV ^{32}S beam hit a 0.44 mg/cm^2 thick ^{28}Si target enriched to 99.1%. It was backed with a 11 mg/cm^2 Ta foil and tilted 30° with respect to the beam to avoid as much screening of the Ge-detectors as possible. To study electromagnetic properties of weak γ-rays in the ^{57}Ni+2pn reaction channel it was necessary to suppress the γ-ray transitions from dominant pure charged-particle evaporation channels, namely ^{54}Fe+1α2p and ^{57}Co+3p. Hence, γ-ray spectra were taken with and without the coincidence with evaporated neutrons. The neutron discrimination employed the pulse-shape analysis of signals coming from a four-fold segmented large-volume NE213 neutron detector positioned at 0°.

The Ge-detector labeled AD was used to measure the angular distribution of γ rays in the range from 0° to 140° relative to the beam direction. (For the two positions at 0° and 20° the neutron detector was removed at the end of the experiment.) The two Ge-detectors M1 and M2, which were fixed at 140°, served as beam current monitors for the angular distribution measurement but also for the determination of angular correlation ratios. M1 was Compton suppressed. The six-fold segmented MINIBALL prototype detector [9,10] P1 and the EUROBALL cluster detector [8, 9] P2 (with suppression shield) at 90° provided the second direction for the angular correlation ratios. Their main purpose, however, was to measure the linear polarization by comparing the count-rates of 'horizontally' and 'vertically' scattered γ rays in two segments or capsules, respectively. Scattering examples are indicated on the right hand side of the figure, which provides the front faces and the numbering of the Cluster elements and the segments, respectively. The detectors AD, M2, P2, and the neutron detector were placed in a horizontal plane with the beam. M1 and P1 were tilted 56° out of that plane. List-mode data was written to magnetic tape if two Ge-crystals and/or two segments of P1 fired. The data comprised a total of 1.7 billion events of which 17% had proper two-fold events within P1, 36% two-fold events within P2, and 43% two- and higher fold coincidences between different Ge-detectors. During the experiment a weak ^{137}Cs source was fixed on the dewar of AD. Finally, energy and efficiency calibration spectra were taken for all seven positions of AD using a ^{226}Ra source.

The normalization factors of the angular distribution analysis were determined to correct for (*i*) different beam currents, (*ii*) different ADC dead times, and (*iii*) different relative efficiencies at the different angle positions of AD by employing (*i*) the intense yrast 3431 keV $8^+ \rightarrow 6^+$ and 411 keV $6^+ \rightarrow 4^+$ transitions in ^{54}Fe [11], (*ii*) the yields of the 661.7 keV line of the ^{137}Cs source, and (*iii*) the extensive ^{226}Ra calibration. The normalization coefficients were tested with strong lines from the ^{32}S+^{28}Si reaction in both AD and M1. The normalized data points were least-squares fitted using the formula [12]

$$W(\theta) = 1 + Q_2 A_2 P_2(cos\theta) + Q_4 A_4 P_4(cos\theta). \quad (1)$$

P_2 and P_4 denote the Legendre polynomials while Q_2 and Q_4 account for the attenuation due to the finite opening angles of the Ge detectors [13].

Since the neutron discrimination and, hence, detection efficiency is count-rate dependent, normalization factors were inferred for the neutron-gated spectra by matching the angular distributions of the two most intense and clean transitions in the neutron-gated spectra, namely the 2577 keV and 1287 keV lines from ^{57}Ni (cf. Fig. 1), in spectra with and without the neutron gate. The result for the 1287 keV line is shown on the left hand side of Fig. 3. Clearly, the lack of data points near 0° for the neutron-gated angular distribution measurement prevents firm conclusions, but the positive A_2 coefficient is consistent with the known stretched $E2$ character. On the right hand side, the 1124 keV transition shows the opposite behaviour, which is consistent with a stretched $\Delta I = 1$ transitions without any admixture of higher multipolarities. Consequently, this result supports the $I = 9/2$ assignment of the 3701 keV level in ^{57}Ni.

Directional correlations of oriented states [14], so called DCO-ratios, were investigated using a $\gamma\gamma$ coincidence ma-

Table 1. Comparison between the average of measured DCO-ratios R(30-83) and R(53-83) [5], here named R(42-83), and the present values R(140-90) for selected γ rays in ^{57}Ni. The suggested multipolarities are given in the fourth row

E_γ (keV)	1075	1100	1124	1136	1287
R(42-83)	1.08(10)	0.38(3)	0.67(8)	0.93(8)	0.97(4)
R(140-90)	1.03(10)	0.44(5)	0.84(10)	0.80(8)	0.98(5)
Mult.	$E2/M1$	$E2/M1$	$E1$	$E2/M1$	$E2$

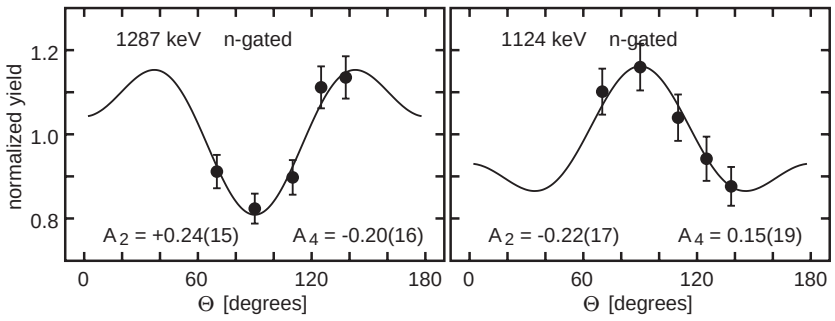

Fig. 3. Angular distributions for the 1287 keV $11/2^- \rightarrow 7/2^-$ and the 1124 keV $9/2^+ \rightarrow 7/2^-$ transitions. The lines are least squares fits to the angular distribution formula (1)

trix with γ rays detected in P1, P2, and AD(90°) and M1, M2, and AD(140°), respectively. The efficiency corrected

$$R_{DCO}(\gamma_1, \gamma_2) = \frac{I(\gamma_1 \text{ at } 140°; \text{ gated with } \gamma_2 \text{ at } 90°)}{I(\gamma_1 \text{ at } 90°; \text{ gated with } \gamma_2 \text{ at } 140°)} \quad (2)$$

ratios are compared to previous results [5] for some transitions in ^{57}Ni in Table 1. The 2577 keV ground-state transition was always used for gating. The value for the 1124 keV line is consistent with a stretched, pure $\Delta I = 1$ transition.

The linear polarization and, consequently, the electric or magnetic character of the radiation can typically (see, e.g., [15]) be determined through a normalized difference of 'horizontally' or 'vertically' Compton scattered γ rays (cf. Fig. 2). Neither the Cluster nor the segmented Ge-detector have the favoured orthogonal configuration (such as, e.g., a EUROBALL Clover detector [16]). Therefore, we define the anisotropy [9,17–19] as

$$A = \frac{\mu N_{\parallel} - N_{\perp}}{\mu N_{\parallel} + N_{\perp}} \quad (3)$$

with $N_{\parallel}$ and $N_{\perp}$ representing the counts of 'vertically' and 'horizontally' scattered γ rays. The coefficient $\mu(E_\gamma)$ can be determined from the ^{226}Ra source calibration. It was found to be 1.52(1) for P1 and 2.01(1) for P2 in the region of interest, i.e., between γ-ray energies 1.0 MeV $< E_\gamma <$ 1.3 MeV. For P2 the coefficient can be readily explained by counting the number of neighboured Cluster element combinations for 'vertical' (4) and 'horizontal' (8) scattering (cf. Fig. 2). For P1 non-neighboured events were also included such as, e.g., segments 1 and 3 for 'horizontal' or segments 2 and 6 for 'vertical' scattering. The non-neighboured segment scatterings provided only 17% of the statistics of neighboured scatterings. Figure 4(a) shows the purified neutron-gated difference and sum spectrum according to the nominator and denominator of (3) using the statistics from P1 and P2. All labeled peaks in the spectra belong to ^{57}Ni (cf. Fig. 1). The 1160, 1227, 1270, and 1287 keV lines are known to be stretched $E2$ transitions. They reveal the expected positive anisotropies for both P1 (c) and P2 (b). The 1075, 1100, and 1136 keV lines are mixed $\Delta I = 1$ transitions with $\delta(E2/M1) = -1.4(8)$, $+0.94(^{18}_{13})$, and -0.15(9) [5], respectively. The positive $E2$ admixture of the 1100 keV nicely coincides with an anisotropy close to zero, while

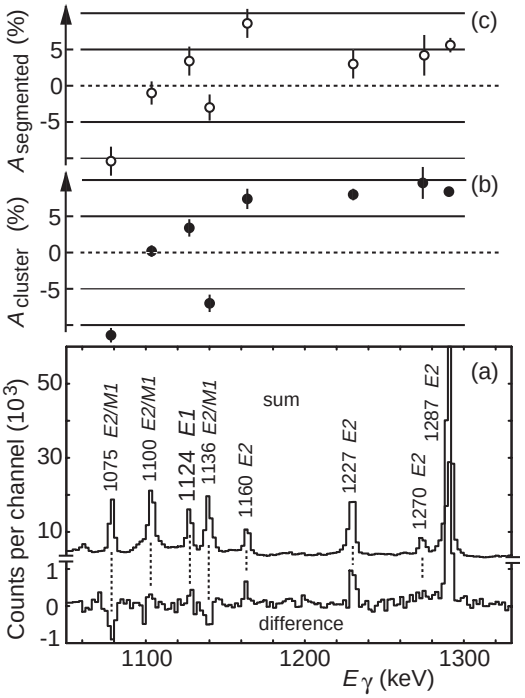

Fig. 4. The γ-ray spectra in part (a) show the normalized difference (bottom) and sum (top) of events scattered parallel or perpendicular to the reaction plane in the Cluster or the segmented Ge-detector. The spectra were measured in coincidence with at least one detected neutron. The lines from pure charged-particle evaporation channels were carefully substracted using identical fractions of the spectra without the neutron coincidence. The peaks are labeled with their energies in keV and their (known) multipole character. The anisotropy (3) measured for these transitions are shown for the Cluster (b) and the segmented Ge-detector (c)

those of the other two $E2/M1$ transitions are negative. A detailed analysis of the polarisation sensitivity of the segmented detector will be published separately [19].

Due to its positive anisotropy and because of a mixing ratio which is consistent with zero we assign the parity-changing $E1$ character to the 1124 keV transition, leading to a spin-parity assigment of $I^\pi = 9/2^+$ for the 3701 keV state. We interpret this state as the neutron $1g_{9/2}$ single-particle state with respect to the doubly-magic core ^{56}Ni.

The authors would like to thank A. Fitzler, D. Gassmann, H. Tiesler, and L. Steinert and his Tandem crew for the support before and during the experiment. This work was supported by the Swedish Natural Science Research Council (NFR) and the German Ministry of Education and Science (BMBF) under contracts 06-GOE-851, 06-OK-862I(0), and 06-LM-868.

References

1. J. Huo, Nucl. Data Sheets **64**, 723 (1991)
2. M.R. Bhat, Nucl. Data Sheets **67**, 195 (1992)
3. C.E. Svensson *et al.*, Phys. Rev. Lett. **82**, 3400 (1999)
4. D. Rudolph *et al.*, Phys. Rev. Lett. **80**, 3018 (1998)
5. D. Rudolph *et al.*, Eur. Phys. J. **A4**, 118 (1999)
6. L. Trache *et al.*, Phys. Rev. C**54** 2361 (1996)
7. J. Duflo and A.P. Zuker, Phys. Rev. C**59** R2347 (1999)
8. J. Eberth, Phys. Blätter **49**, No. 11, 1016 (1993)
9. J. Eberth *et al.*, Prog. Part. Nucl. Phys., Vol. **38**, 29 (1997)
10. D. Habs *et al.*, Prog. Part. Nucl. Phys., Vol. **38**, 111 (1997)
11. J. Huo, H. Sun, W. Zhao, and Q. Zhou, Nucl. Data Sheets **68**, 887 (1993)
12. T. Yamazaki, At. Data Nucl. Data Tables **3**, 1 (1967)
13. D.C. Camp and A.L. van Lehn, Nucl. Instr. Meth. **76**, 192 (1969)
14. K.S. Krane, R.M. Steffen, and R.M. Wheeler, At. Data Nucl. Data Tables **11**, 351 (1973)
15. W.D. Hamilton, *The Electromagnetic Interaction in Nuclear Spectroscopy*, North-Holland, Amsterdam, 1975
16. P.M. Jones *et al.*, Nucl. Instr. Meth. **A357**, 458 (1995)
17. L.M. Garcia-Raffi *et al.*, Nucl. Instr. Meth. **A359**, 628 (1995)
18. D. Weisshaar, Diploma thesis, Cologne 1996, unpublished
19. D. Weisshaar *et al.*, to be published